Low-cost Energy Measurement and Estimation for Autonomous Underwater Vehicles

Valerio De Carolis, David M. Lane and Keith E. Brown
Ocean System Laboratory, School of Engineering & Physical Sciences
Heriot-Watt University, EH14 4AS, Edinburgh, UK
Email: vd63@hw.ac.uk

***Abstract*—This work introduces a low-cost energy measurement method and proposes a simple linear model to estimate the vehicle energy consumption when navigating a given trajectory. Experimental results on Nessie VII AUV show that the developed system can be used to measure the energy used during the vehicle's operations with a good confidence level. Moreover the proposed estimation model can be trained using a simple calibration procedure each time the environmental conditions change or the vehicle's configuration is altered. The proposed solution is suited to real-time use on low-power embedded devices. The limited use of computation resources mean that this method is well suited for supporting navigation planning and motion control.**

I. Introduction

Energy-awareness is a well-known problem in the autonomous vehicles research community. With the increase of the complexity and duration of missions the correct use of the on-board resources is becoming a fundamental aspect especially for the autonomous systems, which aim to provide higher performances in terms of reliability, long-term operability, adaptation and persistent autonomy. This is particularly true for today autonomous underwater vehicles (AUVs) and for their missions where the operating environment, the payload and the space constraints set strict constraints on vehicle's design and mission planning. The idea of getting a qualitative estimation of potential vehicle range given the energy stored in vehicle's batteries has been already explored in the past. Using a simple metric, like the one proposed in [1], to provide such estimation is effective especially when the power requirements of total load can be assumed fixed and when most of the mission's time is spent navigating along a given trajectory maintaining a constant energy usage. On the other hand when considering a different set of missions, like inspection of human-made underwater structures or maintenance tasks [2], the assumption made above cannot be made, especially when the AUV is equipped with advanced planning capabilities that adapt and plan the future tasks according to the acquired knowledge and the mission's rules.

Deployment under energy and time constraints has been initially studied ([3], [4]) for groups of mobile robots and then extended to other classes of autonomous vehicles. Some work has been done to analyse and predict the mission's energy usage [5] for unmanned ground vehicles (UGV) and comparing the navigation and guidance algorithm analysis [6] for unmanned aerial vehicles (UAV) using energy expenditure as a benchmark metric. Mission adaptation in dynamic environments [7] has been analysed in detail for long-endurance AUVs using the same constraints.

The work presented in the following sections introduces the energy measurement solution we developed for our research vehicle, Nessie VII [8]. Nessie VII is a torpedo-shaped hover-capable AUV which has been developed in the Ocean Systems Laboratory and used for a variety of research experiments. The vehicle has been upgraded with four Li-Ion batteries, providing 2.2 kWh of energy, and six brushless DC thrusters, each of them capable of developing up to 250 W of power. In its latest configuration two new sonars have been added. One of them, externally attached, uses a pan and tilt unit for use in inspection tasks and fitted only when this capability is needed. The energy measurement solution we developed for Nessie VII

Figure 1. Nessie VII AUV during pre-trial testing inside OSL facilities. The pan-and-tilt unit with sonar has been fitted underneath the vehicle to provide enhanced capabilities for inspection and surveying tasks.

proposes a simple energy estimation model that was derived and used for navigation planning and motion control. Because of its simplicity, the proposed model can be adjusted before starting a new mission using a short calibration procedure to adapt the model coefficients to different external payload configurations which can introduce effects (increased inertia and drag) on vehicle navigation. Despite providing only basic measurements and estimations this work is intended to be a first building block for a fully integrated system capable of providing diagnostic information and fault detection while at the same time collecting data on how the resources are being used, on how much resource is still available for subsequent tasks, on how well these resources are being used.

II. Current Sensing

Nessie VII did not have the capability of measuring energy consumption. Some of the internal components, like thrusters, can already provide a rough estimation of their current consumption but often their accuracy and precision is not known or they rely on proprietary solutions for accessing raw measurements. In addition the direct measurement of energy consumption opens up opportunities for improved fault diagnosis systems. With the aim of introducing a low-cost solution and avoiding relying on a specific thruster model we decided to directly integrate a current sensing device [9] on the vehicle's main electrical bus. We implemented a simple coulomb-counting procedure to measure the energy used by the entire platform. Most of the sensing devices are able to convert directly the current flow into an output voltage. By using an ADC this output can be converted to a current measurement a_{sense} by applying the sensor's model, usually linear when operating within a given range. After analysing the operating condition and the internal design of Nessie VII a Hall-effect based sensor was selected. The sensor can work on wide operational range (0A to 30A) while providing optimal decoupling [10] between the high voltage main bus and the low voltage data acquisition devices. Because of the sensing device placement (before any load but near the battery bus) such a system is also used to estimate the depth-of-discharge of the vehicle's battery. In this manner we gain extra information about the battery state along with existing level indicators already integrated inside the vehicle.

$$E[T] = \sum_{n=0}^{T} dE[n] \tag{1}$$

The energy usage is then calculated by integration (1) of the sensed current values. Those are acquired at a fixed sampling rate $F_s = 1/T_s$ using a dedicated microcontroller (MCU) device and then processed by main vehicle's computer. To achieve good precision a trapezoidal approximation is used:

$$E[T] = \sum_{n=1}^{T} V_{bus} \frac{a_{sense}[n-1] + a_{sense}[n]}{2} \; T_s \tag{2}$$

where V_{bus} is main bus voltage, T_s is the sampling time, a_{sense} the measured current amplitude and T represents the time of measurement on a sampled-time axis.

III. Energy Estimation

Estimating the energy consumption for a moving vehicle along a given trajectory is a difficult task as described in [5] and [11]. This is especially true when few assumptions can be made of the operating environment. In the underwater vehicle domain the presence of a high number of degrees of freedom (DOF) and the high variability of operating conditions represent a difficult challenge when providing such estimation. This is because several aspects should be evaluated, like the effect of external disturbances [12], often not taken into account in the hydrodynamic models, and the operation of the advanced controllers (cascaded PID loops or robust control designs) which often are used in such vehicles. Part of this work is developed with the specific aim of abstracting from the underlying control architecture, which could be effectively part of a separate subsystem, while only analysing its effects on the vehicle navigation. Despite the possibility of using the hydrodynamic model to estimate ahead-of-time the actual motion of the autonomous platform this work has also the goal of keeping the computational complexity low enough to allow extensive use of the prediction model with an external trajectory planner and within the vehicle motion control module when selecting a low-energy path.

A. Linear Model

We are proposing a linear model that is used to estimate the required energy for navigating along a known trajectory. This is given as an ordered list of the waypoints described by a 6DOF vector in north-east-depth-roll-pitch-yaw (NEDRPY) reference system. The trajectory is then analysed piecewise, considering pairs of consecutive waypoints as the basic input for the energy model. Given a pair of waypoints w_A and w_B in NEDRPY reference, a displacement vector D can be calculated in body-frame (BF) reference by a simple rotation transform using the vehicle attitude at the initial waypoint:

$$D_{AB} = [\Delta_x \; \Delta_y \; \Delta_d \; \Delta_\phi \; \Delta_\theta \; \Delta_\psi]^T \tag{3}$$

where the first three terms, Δ_x, Δ_y, Δ_d, represent the coordinate change on the longitudinal, lateral, vertical axes and the last three, Δ_ϕ, Δ_θ, Δ_ψ, the rotations around the same axes. Each delta is then used in a linear combination of terms to estimate the required energy Δ_E to move the AUV between the two waypoints:

$$\Delta_E(w_A, w_B) = k_1\Delta_x + k_2\Delta_y + k_3\Delta_d + k_4\Delta_\psi \tag{4}$$

Since we are not actively controlling the pitch and roll in our experimental setup the Δ_ϕ and Δ_θ terms are explicitly removed from model. According to observed data, displacements along x, y, z axes as well as yaw rotations can be approximated by a linear term as outlined in (4). The total energy estimation is then calculated for the N-waypoint trajectory as the sum of $N-1$ individual legs, assuming w_0 the initial waypoint:

$$T_{energy} = \sum_{i=1}^{N} \Delta_E(w_{i-1}, w_i) \qquad i = 0, 1, \ldots, N \tag{5}$$

The BF coordinate reference system is used instead of the NED one because by its nature it is aligned to vehicle's principal axis, making the displacement along x and y axis, respectively surge and sway movements, relative only to pairs of homogeneous thrusters for our target configuration.

$$w_A = [n \; e \; d \; \phi \; \theta \; \psi]^T \tag{6}$$

The waypoint w_A in NED reference, where n, e, d, ϕ, θ, ψ represent respectively north, east, depth coordinates and pitch, roll, yaw attitude angles. Because we are interested in the relative position of waypoint w_B respect to w_A the two of them can be rewritten in body-frame reference as:

$$p_A = [x_a \; y_a \; d_a \; \phi_a \; \theta_a \; \psi_a]^T \tag{7}$$

$$p_B = [x_b \; y_b \; d_b \; \phi_b \; \theta_b \; \psi_b]^T \tag{8}$$

where the north and east coordinates are replaced with body-frame ones using the rotation transform defined by M matrix:

$$[x \; y]^T = M \; [n \; e]^T \tag{9}$$

The rotation matrix M is calculated using the vehicle attitude at w_A waypoint considering a simple geometry:

$$M = \begin{bmatrix} \cos(\phi)\cos(\psi) & \cos(\theta)\sin(\psi)+\sin(\theta)\sin(\phi)\cos(\psi) \\ -cos(\phi)\sin(\psi) & \cos(\theta)\cos(\psi)-\sin(\theta)\sin(\phi)\sin(\psi) \end{bmatrix} \quad (10)$$

After applying the transformation to both waypoints one can calculate the displacement vector $D = |p_A - p_B|$ by difference, obtaining the relative change of position and attitude for the given trajectory leg.

B. Model Calibration

The coefficients $k_1, \ldots, k_n$ in (4) are calculated individually using the least-square fitting method on recorded data when navigating on given trajectories, designed to stimulate one degree of freedom at time. Considering the configuration of Nessie VII we decided to test extensively the surge, sway, heave and yaw degree-of-freedom by generating trajectories where all but the tested degree of freedom is kept constant. For instance, when stimulating the *surge* DOF the calibration trajectory W_{surge} has been generated according (12), where d is an offset and L is the minimum distance between consecutive waypoints.

$$W_{surge} = \begin{bmatrix} x_{surge}(0) & 0 & \cdots & 0 \\ x_{surge}(1) & 0 & \cdots & 0 \\ \vdots & \vdots & \cdots & \vdots \\ x_{surge}(N) & 0 & \cdots & 0 \end{bmatrix} \quad \text{N > 0} \quad (11)$$

$$x_{surge}(n) = \begin{cases} 0 & \text{if } n \text{ is even} \\ d + (n-1)L & \text{if } n \text{ is odd} \end{cases} \quad (12)$$

In this way the writing of displacement vector D_{surge} can be reduced to a single component which is then used for fitting the k_1 coefficient.

$$D_{surge} = \begin{bmatrix} \Delta_{x_1} = x_1 - x_0 \\ \vdots \\ \Delta_{x_N} \end{bmatrix} \quad (13)$$

The energy vector Δ_E, instead, is calculated taking into account the difference of total energy usage (2) between consecutive waypoints.

$$\Delta_{E_{surge}} = \begin{bmatrix} \Delta_{E_1} = E\left[T_1\right] - E\left[T_0\right] \\ \vdots \\ \Delta_{E_N} \end{bmatrix} \quad (14)$$

After computing the two vectors D and Δ_E a least-square fitting can be applied thus calculating the k_1 coefficient related to surge displacement.

$$\Delta_{E_{surge}} = k_1 \; D_{surge} \quad (15)$$

This calibration procedure then is applied again for the others DOFs obtaining the full set of coefficients for a given vehicle configuration. For Nessie VII AUV the following relation has been found after calibrating the linear model:

$$k_1 > k_2 > k_4 \quad (16)$$

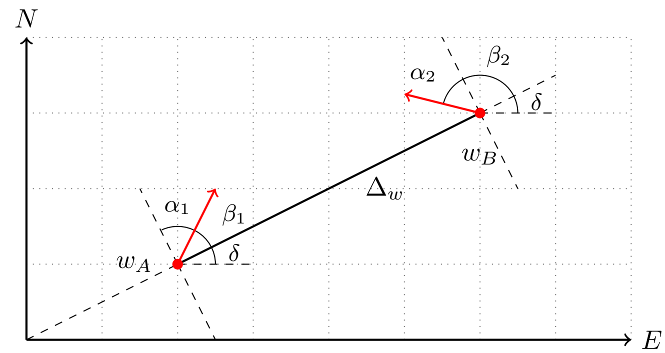

Figure 2. Geometric representation of two waypoints (w_A, w_B) with required yaw attitude in north-east plane. The angles α and β represent the orientation changes needed respectively for *forward* and *lateral* navigation modes while δ is the line-of-sight angle between waypoints.

C. Guidance Optimization

Once the model has been fitted a simple guidance rule, that has been derived, is used to select the most appropriate guidance mode between *forward navigation* (FNAV) and *lateral navigation* (LNAV). In the former mode the vehicle needs to adjust its attitude to navigate towards the next waypoint by moving forward thus using mostly the forward thrusters. In the latter the adjustment is made to use lateral thrusters thus rotating the vehicle to be orthogonal to the path among waypoints. To select the guidance mode a software module in the vehicle estimates the cost of two modes and chooses the cheapest alternative:

$$E_{FNAV} = k_1\Delta_w + k_4\beta_1 + k_4\beta_2 \quad (17)$$
$$E_{LNAV} = k_2\Delta_w + k_4\alpha_1 + k_4\alpha_2 \quad (18)$$

where Δ_w is distance between waypoints, (α_1, α_2) and (β_1, β_2) are rotation angles for the two guidance modes, shown in Figure 2. This has been shown to be effective when the vehicle is navigating on trajectories with short legs and a high number of attitude changes, for instance while performing an inspection task, to orientate the sensors and acquire the data. In this case the vehicle can consider the *lateral navigation* as an alternative to *forward* mode if the associated rotation's cost is lower and the distance between waypoints is short. More generally a separation rule can be derived directly by comparing the (17) and (18) in the worst-case scenario[1] of *forward navigation* and considering the relationship (16) among coefficients of Nessie VII AUV:

$$\Delta_w \leq \frac{k_4\pi}{k_2 - k_1} \quad (19)$$

The (19) suggests that below a given waypoints' distance can be convenient to consider a different guidance mode other than the *forward navigation* for an energy-efficient point of view.

IV. Experimental Results

Initial experiments have been conducted using the UWSim simulator [13] together with the Nessie VII hydrodynamic and

[1]The worst-case FNAV scenario is where the *forward navigation* guidance requires the maximum attitude changes compared to the one needed by LNAV. This can be seen in Figure 2 when $\alpha_1 = \alpha_2 = \pi$ and $\beta_1 = \beta_2 = \pi/2$.

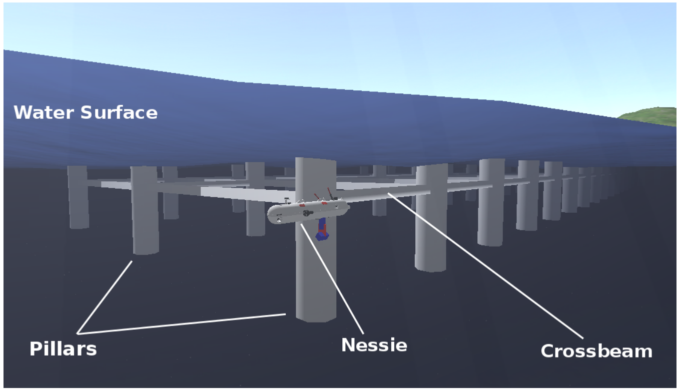

Figure 3. Underwater view of the simulated mission's scenario. The structure to inspect is made by concrete pillars and crossbeams. Nessie VII AUV is collecting data from its sensors while navigating around pillars.

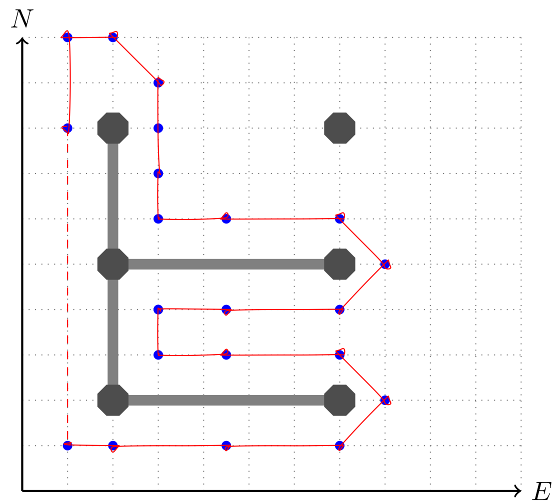

Figure 4. Nessie AUV trajectory plan in north-east plane for an inspection mission around human-made structures. The blue dots represents the trajectory's waypoints while the red line the real navigation path. The inspected structure, made of concrete pillars and crossbeams, is represented in grey.

thrusters model. The use of the simulator enabled us to test the proposed approach with different types of mission and trajectories before deploying new software inside the vehicle itself. Despite the presence of a simulated environment the use of Robot Operative System (ROS) [14] framework enabled us to conduct the series of experiments using the same software, like control and navigation modules, already deployed inside the vehicle.

Table I. INSPECTION MISSION DETAILS

Mission Details	
Total Duration	340.86 s
Total Navigation Distance	86.07 m
Total Energy Usage	35.56 Wh
Battery Initial Capacity	1800 Wh
Battery Usage	2.03 %

Several scenarios have been simulated, we chose a particular inspection mission as our reference test-case because this will provide enough knowledge to validate the proposed work in the next field trials scheduled in the summer. Such missions require the vehicle to survey the underwater section of a pier, as shown in Figure 3, to collect data from several concrete elements like pillars and crossbeams supporting the pier's structure above.

Table II. MODEL CALIBRATION COEFFICIENTS

Coefficient	Value
k_1	557.24 J/m
k_2	1174.21 J/m
k_3	1118.13 J/m
k_4	1607.14 J/rad

Nessie VII AUV is instructed to inspect a section of the underwater structure following an input trajectory, like the one represented in Figure 4, by providing a list of inspection waypoints. To evaluate the efficiency of the proposed work we compared the vehicle energy usage, calculated using Nessie's thruster model directly from simulated navigation, with the estimated energy for the inspection task's trajectory using the model we introduced in the previous sections.

Before deploying the proposed work in the vehicle platform a new software module has been implemented to derive

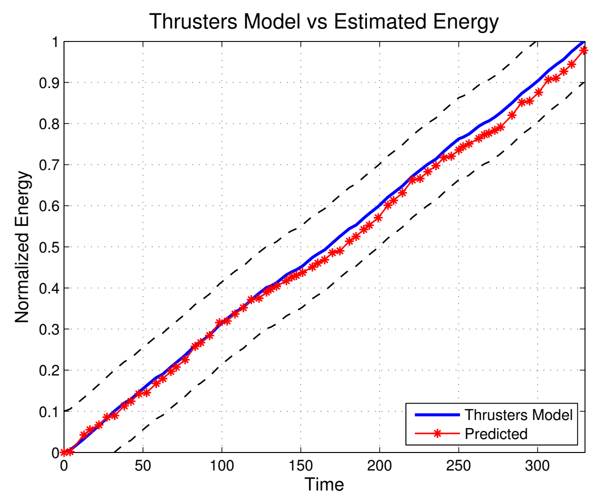

Figure 5. Comparison between thruster's model and predicted energy using the proposed model for inspection mission. The energy values have been normalised to the total resource usage for the final navigation trajectory.

Table III. ENERGY ESTIMATION DETAILS

Energy Estimation	
Measured Energy Usage	35.56 Wh
Predicted Energy Usage	34.18 Wh
Prediction Error	3.89 %

the energy usage inside the simulated UWSim environment. Using the speed of thrusters, requested by the pilot module during navigation, and applying the thruster's model, already known from previous experiments, the new module is able to calculate the total current usage of Nessie's thrusters. Using the computed values we derived the vehicle's energy usage and used it as reference to evaluate the quality of the proposed energy estimation model. Results, shown in Figure 5, have been normalised to the thrusters' energy to highlight the difference between predicted and reference values along the entire vehicle's trajectory. After completing the inspection task we compared the total energy usage to the estimated one, that was calculated before starting the navigation, as shown in Table III. Using the proposed model we were able to predict the energy requirements within 10% of total usage for the given task. This result shows that we are able to achieve a good correlation between the proposed approach and the thruster's model already analysed during previous experiments. Moreover this gives us enough confidence to use this tool to monitor the execution of tasks in complex missions to further validate the model with real mission data.

V. Conclusions

Offline simulation results have suggested we should expect a good confidence level for operation in a shallow water without strong sea currents. This method is particularly attractive for use with a trajectory or motion planner, because of its low computational requirements, giving the possibility of using the forward-predicted energy as a cost function to select the best guidance mode from the available ones without requiring an excessive computational cost, typical of an hydrodynamic simulation method. While forward prediction is a useful tool to look at near future in the mission's time line, this method can find application in analysing the recent past during a mission's execution and after completing a given set of task. A dedicated software module can compare the real energy usage of a completed task to the expected usage that is calculated from known models. This provides more information in cases where there is the presence of a noticeable difference, for instance because of changes in the external environment or undetected misbehaviours with platform's payload. For these reasons the proposed work has to be intended as first element of a more integrated energy management system, currently underdevelopment, which, will be presented in the future. Such a system has the goal to provide a sufficient level of energy-awareness to extend vehicle's self-management capabilities, to provide a better understanding of the resource usage during the mission execution and to collect all the necessary information to build a knowledge base that will be used during mission planning and execution.

Acknowledgement

The authors would like to thank all the other members of the Ocean Systems Laboratory at Heriot-Watt University. The research leading to these results has received funding from the European Union Seventh Framework Programme FP7/2007-2013 - Challenge 2 - Cognitive Systems, Interaction, Robotics - under grant agreement No 288273 - PANDORA.

References

[1] A. Bradley, M. Feezor, H. Singh, and F. Yates Sorrell, "Power systems for autonomous underwater vehicles," *IEEE Journal of Oceanic Engineering*, vol. 26, no. 4, pp. 526–538, 2001.

[2] D. M. Lane, F. Maurelli, T. Larkworthy, D. Caldwell, J. Salvi, M. Fox, and K. Kyriakopoulos, "Pandora: Persistent autonomy through learning, adaptation, observation and re-planning," in *Proceedings of IFAC NGCUV 2012 - Navigation, Guidance and Control of Underwater Vehicles*, 2012.

[3] F. Dressler and G. Fuchs, "Energy-aware operation and task allocation of autonomous robots," *Robot Motion and Control, 2005*, pp. 163–168, 2005.

[4] Y. Mei, S. Member, Y.-h. Lu, Y. C. Hu, and C. S. G. Lee, "Deployment of Mobile Robots With Energy and Timing Constraints," vol. 22, no. 3, pp. 507–522, 2006.

[5] A. Sadrpour, J. Jin, A. G. Ulsoy, and S. Member, "Mission Energy Prediction for Unmanned Ground Vehicles," pp. 2229–2234, 2012.

[6] O. Spinka and Z. Hanzalek, "Energy-Aware Navigation and Guidance Algorithms for Unmanned Aerial Vehicles," *2011 IEEE 17th International Conference on Embedded and Real-Time Computing Systems and Applications*, pp. 83–88, Aug. 2011.

[7] M. L. Seto, "On-line Learning with Evolutionary Algorithms towards Adaptation of Underwater Vehicle Missions to Dynamic Ocean Environments," *2011 10th International Conference on Machine Learning and Applications and Workshops*, pp. 235–240, Dec. 2011.

[8] N. Valeyrie, F. Maurelli, P Patron, J. Cartwright, B. Davis, Y. Petillot, "Nessie v turbo: a new hover and power slide capable torpedo shaped auv for survey, inspection and intervention," in *AUVSI North America 2010 Conference*, 2010.

[9] C. Xiao, L. Zhao, T. Asada, W. Odendaal, and J. Van Wyk, "An overview of integratable current sensor technologies," in *Industry Applications Conference, 2003. 38th IAS Annual Meeting. Conference Record of the*, vol. 2, 2003, pp. 1251–1258 vol.2.

[10] K. Yang and H. Amplifiers, "Advanced Current Sensing Suits High-Rel Systems," *Power Electronics*, no. August, 2005.

[11] M. Chyba, T. Haberkorn, S. Singh, R. Smith, and S. Choi, "Increasing underwater vehicle autonomy by reducing energy consumption," *Ocean Engineering*, vol. 36, no. 1, pp. 62–73, Jan. 2009.

[12] P. Kormushev and D. Caldwell, "Improving the energy efficiency of autonomous underwater vehicles by learning to model disturbances," *Intelligent Robots and Systems*, 2013.

[13] M. Prats, J. Perez, J. Fernandez, and P. Sanz, "An open source tool for simulation and supervision of underwater intervention missions," in *Intelligent Robots and Systems (IROS), 2012 IEEE/RSJ International Conference on*, 2012, pp. 2577–2582.

[14] M. Quigley, K. Conley, B. Gerkey, J. Faust, T. Foote, J. Leibs, R. Wheeler, and A. Y. Ng, "Ros: an open-source robot operating system," in *ICRA workshop on open source software*, vol. 3, no. 3.2, 2009.